Research Article

Journal of Physical Organic Chemistry

Received: 1 January 2008, Revised: 27 March 2008, Accepted: 20 July 2008, Published online in Wiley InterScience: 3 November 2008

(www.interscience.wiley.com) DOI 10.1002/poc.1434

Structural, electronic, and optical properties of oligoquinolines for light-emitting diodes

Lei-Jiao Li[a], Ji-Kang Feng[a,b]* and Ai-Min Ren[a]

The purpose of this work is to provide an in-depth investigation of the electronic and optical properties of a series of *n*-type conjugated oligomers, including 4-phenyl-6-(4-phenylquinolin-6-yl)quinoline (B1), 6,6′-bis(2,4-diphenylquinoline) (B1PPQ), 6,6′-bis(2-(4-*tert*-butylphenyl)-4-phenylquinoline) (BtBPQ), 6,6′-bis(2-*p*-biphenyl)-4-phenylquinoline) (B2PPQ), and 4-(6-(2-(4-aminophenyl)-4-phenylquinolin-6-yl)-4-phenylquinolin-2-yl)benzenamine (BNPPQ). The geometric and electronic structures of the oligomers in the ground state were investigated using density functional theory (DFT) and the *ab initio* HF, whereas the lowest singlet excited states were optimized with *ab initio* CIS. To assign the absorption and emission peaks observed in the experiment, we computed the energies of the lowest singlet excited states with time-dependent (TD) DFT (TD-DFT). All DFT calculations were performed using the B3LYP functional and the 6-31G basis set. The results show that the HOMOs, LUMOs, energies gaps, ionization potentials and electron affinities for each molecular are significantly affected by varying the aryl substituents, which favor the hole injection into OLEDs. The absorption and emission spectra exhibit red shifts to some extent [the absorption spectra: 335.85 (B1)< 370.63 (B1PPQ) < 376.77 (BtBPQ)< 388.67 (B2PPQ)< 412.93 nm (BNPPQ); the emission spectra: 391.48 (B1)< 430.11 (B1PPQ)< 435.86 (BtBPQ)< 444.57 (B2PPQ)< 463.28nm (BNPPQ)]. The radiative lifetimes (τ) of each oligomers are calculated as well. Because of introducing the cooperation with the electron donators such as the amidocyanogen in the common 4-phenyl-6-(4-phenylquinolin-6-yl)quinoline core for BNPPQ, which results in improving the hole-creating ability. Copyright © 2008 John Wiley & Sons, Ltd.

Keywords: OLEDs; oligoquinolines; TDDFT

INTRODUCTION

The *n*-type conjugated oligomers constitute an active component of organic light emitting diodes (OLEDs) since they exhibit unique and interesting optoelectronic properties.[1–8] As a result, a wide range of functionalized *n*-type conjugated oligomers have been designed and synthesized to tune the desirable optical and electronic properties and to enhance the processing and morphological properties. However, the highly efficient π-stacking interactions of the *n*-type conjugated oligomers in solid state significantly reduced their photoluminescence (PL) quantum yields and shifted their emission spectra to yellow, orange, and red ranges.[9–12] So some new blue light-emitting organic materials are also needed for developing high-performance blue OLEDs.

In parallel to recent experimental work on the oligomers, theoretical efforts have indeed begun to constitute an important source of valuable information, complementing the experimental studies in the characterization of the nature and the properties of the ground-states and lowest electronic excited states.[13–18] Here, we investigated in detail five *n*-type conjugated oligomers (the sketch map of the structures is depicted in Fig. 1) which have a common 4-phenyl-6-(4-phenylquinolin-6-yl)quinoline core and various aryl substituents at both ends. The theoretical investigation on the ionization potentials (IP), electron affinities (EAs), and band gaps of these molecules is very instrumental in guiding the experimental synthesis. In particular, the influence of substitution on various optical and electronic properties is the topic of the present work.

COMPUTATIONAL DETAILS

In the calculation, C_2 symmetry is adopted to settle the conformations of all the models both in the ground and the excited states. The ground-state geometries as well as their cationic and anionic geometries were fully optimized using the DFT//B3LYP/6-31G. It has been reported in the literature[19,20] that the 6-31G basic set yields a similar result on the prediction of dihedral angle of conjugated materials as that of 6-31G* (6-31G* basic set with added augmentation of polarization function). Since the calculation of B3LYP/6-31G* is time-consuming for conjugated oligomers, the 6-31G is chosen as the basic set for the present study. Based on the optimized ground-state structures calculated by *ab initio* HF/6-31G method, the lowest singlet excited-state structures were carried out with *ab initio* CIS/6-31G. We have used time-dependent density functional theory

* *Correspondence to: J.-K. State Key Laboratory of Theoretical and Computational Chemistry, Institute of Theoretical Chemistry, Jilin University, Changchun 130023, People's Republic of China.*
E-mail: JiKangf@yahoo.com

a *L.-J. Li, J.-K. Feng, A.-M. Ren*
State Key Laboratory of Theoretical and Computational Chemistry, Institute of Theoretical Chemistry, Jilin University, Changchun 130023, People's Republic of China

b *J.-K. Feng*
The College of Chemistry, Jilin University, Changchun 130023, People's Republic of China

Journal of Physical Organic Chemistry

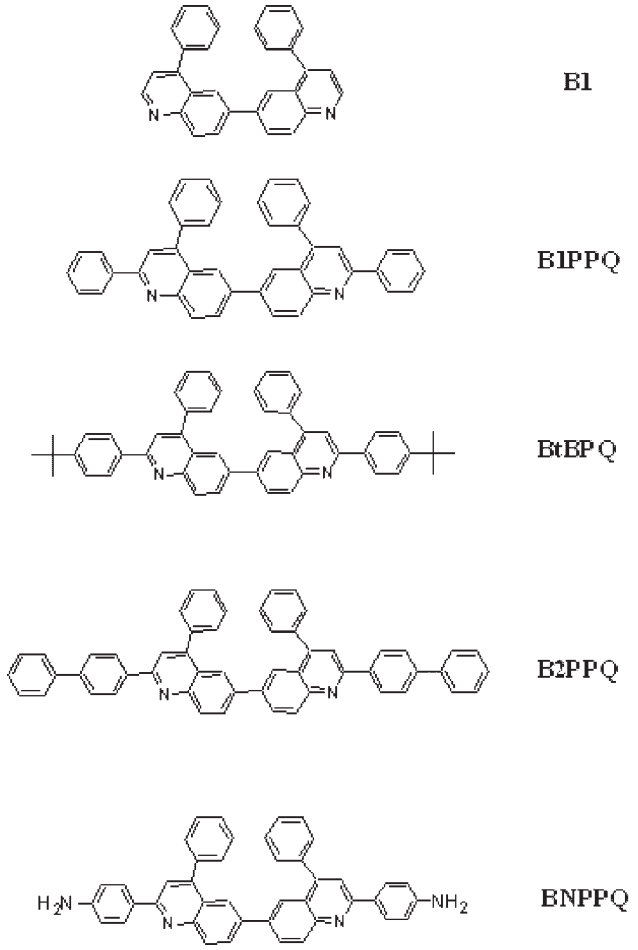

Figure 1. Sketch structures of five oligoquinolines

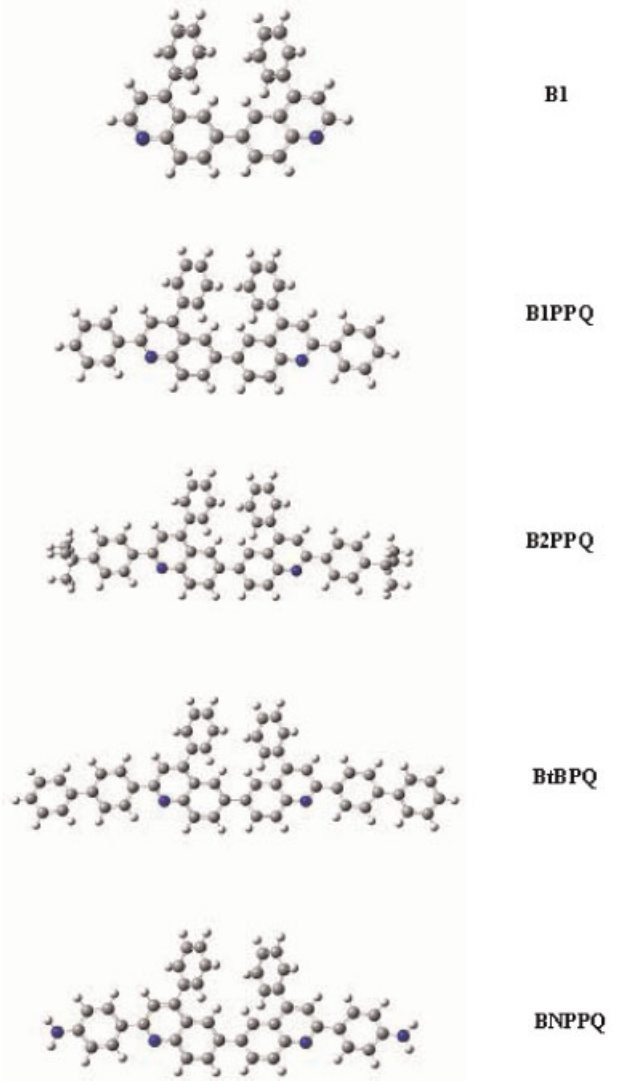

Figure 2. Optimized structures of B1, B1PPQ, BtBPQ, B2PPQ, and BNPPQ by DFT//B3LYP/6-31G

(TD-DFT) as it has previously been shown to be applicable for calculations of both absorption and emission properties for a large number of molecules.[21,22] In addition, the various properties of the oligomers, such as IP, EA, HOMO-LUMO gap (Δ_{H-L}), optical band gap (E_g), and the decay lifetimes (τ), were obtained from the computed results and compared to the available experimental data. All calculations were done on the SGI origin 2000 server with the Gaussian03 program package.[23]

RESULTS AND DISCUSSION

Ground-state and excited-state structures

The optimized structures of these oligomers calculated by DFT//B3LYP/6-31G are depicted in Fig. 2. And the elected bond lengths and twist angles are collected in Table 1. For the sake of comparison of the ground and excited structures, a part of bond lengths and twist angles of the excited structures for these quinoline oligomers with CIS/6-31G are also list in Table 1.

In the ground state, the DFT calculated results are similar to those obtained with the HF approach except the twist angles, which are overestimated by HF method. Both oligomers show similar torsion angles between the bis(quinoline) units at about 37° (DFT//B3LYP/6-31G) and 44° (HF/6-31G). The 2-phenyl groups of 6,6′-bis(2,4-diphenylquinoline) (B1PPQ) are distorted at angles of 11.9° relative to the quinoline moiety, whereas these are 11 and 23° in experiment. The 2-(4-tert-butylphenyl) groups of 6,6′-bis(2-(4-*tert*-butylphenyl)-4-phenylquinoline) (BtBPQ) are distorted 6.1°, whereas the experimental data are 27 and 36°. Additionally, the 4-phenyl groups of B1PPQ are distorted by 53.7°, and these are 49 and 61° in experiment. These angles are 53.9° in BtBPQ compared to 58 and 63° in experiment. In fact, it is difficult to compare the computed and experimental inter-ring angles, because the rotational disorder was ruled out by optimizing the structures and the experimental values were measured in the solid state. Table 1 listes the influence of different substitutions on the geometry. The presence of these different substitutions on the common 4-phenyl-6-(4-phenylquinolin-6-yl)quinoline core leads to only small changes in the inter-ring distances and bond angles. The bond lengths [see bonds C(1)-C(2) and C(5)-C(6)] show a slight alternation at about 0.001 Å. The largest change occurs for the twist angles between the two substitutions and the 4-phenyl-6-(4-phenylquinolin-6-yl)quinoline core. The twist angles are similar for B1PPQ (11.9°), 6,6′-bis(2-*p*-biphenyl)-4-phenylquinoline) (B2PPQ) (6.1°), and BtBPQ (7.0°), but a little

Table 1. Selected bond lengths and dihedral angles for B1, B1PPQ, BtBPQ, B2PPQ and BNBPQ in ground state and the excited state

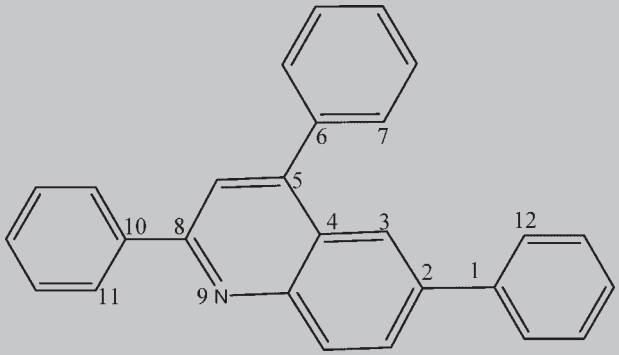

	Interring distances (Å)			Dihedral angles (°)			Dipole moment (*D*)
	C(1)–C(2)	C(5)–C(6)	C(8)–C(10)	C(4)–C(5)–C(6)–C(7)	N(9)–C(8)–C(10)–C(11)	C(12)–C(1)–C(2)–C(3)	
DFT//B3LYP/6-31G							
B1	1.487	1.489	—	54.8	—	37.8	4.523
B1PPQ	1.486	1.490	1.486	53.7	11.9	37.6	3.811
BtBPQ	1.485	1.490	1.485	53.9	6.1	38.0	3.673
B2PPQ	1.486	1.490	1.484	53.9	7.0	37.6	3.764
BNPPQ	1.485	1.490	1.479	54.1	4.5	37.3	3.120
HF/6-31G							
B1	1.488	1.492		63.4		45.1	4.713
B1PPQ	1.487	1.492	1.485	62.9	22.5	44.7	3.991
BtBPQ	1.487	1.492	1.483	62.9	20.9	44.6	3.845
B2PPQ	1.487	1.492	1.484	63.0	21.0	44.7	3.955
BNPPQ	1.487	1.493	1.479	63.0	16.5	44.5	3.523
CIS/6-31G							
B1	1.425	1.483	—	52.7	—	5.4	5.232
B1PPQ	1.428	1.487	1.469	56.1	6.6	7.5	4.414
BtBPQ	1.428	1.487	1.465	56.6	3.5	7.8	4.207
B2PPQ	1.430	1.487	1.463	57.4	1.6	8.5	4.339
BNPPQ	1.430	1.488	1.459	57.1	1.7	9.0	3.722

smaller for 4-(6-(2-(4-aminophenyl)-4-phenylquinolin-6-yl)-4-phenylquinolin-2-yl)benzenamine (BNPPQ) (4.5°). This difference should be a result of the smaller steric hindrance in BNPPQ. All the results suggest that these quinoline derivatives have nonplanar molecular structures. These structures features are of interest because they could reduce the π-stacking interaction and the likelihood of excimer formation in solid films.

The electronic excitation leads to the varieties of the oligoquinolines' structures as shown in the values calculated by HF and CIS approaches. The bonds C(1)—C(2) are shortened by about 0.06 Å, whereas the bonds C(5)—C(6) are shortened by only 0.005 Å. The C(8)—C(10) are also shortened a little. As expected, the twist angles of these quinoline derivatives greatly vary. The torsion angles between the bis(quinoline) units are 5.4, 7.5, 7.8, 8.5, and 9.0°, respectively. This indicates that the singlet excited states should be much more planar than their ground states.

The dipole moment values for these quinoline derivatives are also listed in Table 1. As observed earlier, the HF data are higher than those calculated by DFT in the ground state. In addition, we find that the dipole moments of each oligomer in the excited state are higher than those in the ground state from Table 1.

Frontier molecular orbitals

Interestingly, the main characteristics of the frontier orbitals by HF/6-31G are similar to ones by DFT//B3LYP/6-31G. To gain insight into the excitation properties and the ability of electron or hole transport, we have drawn the HOMOs and LUMOs of B1, B1PPQ, BtBPQ, B2PPQ, and BNPPQ by DFT in Fig. 3.

As visualized in Fig. 3, the frontier orbitals show π characters and spread over the whole conjugated molecules. These oligomers show similar characters as shown in the figure. In general, the HOMO possesses bonding character and LUMO holds antibonding character. There is antibonding between the bridge atoms of the inter-ring, and there is bonding between

Journal of Physical Organic Chemistry

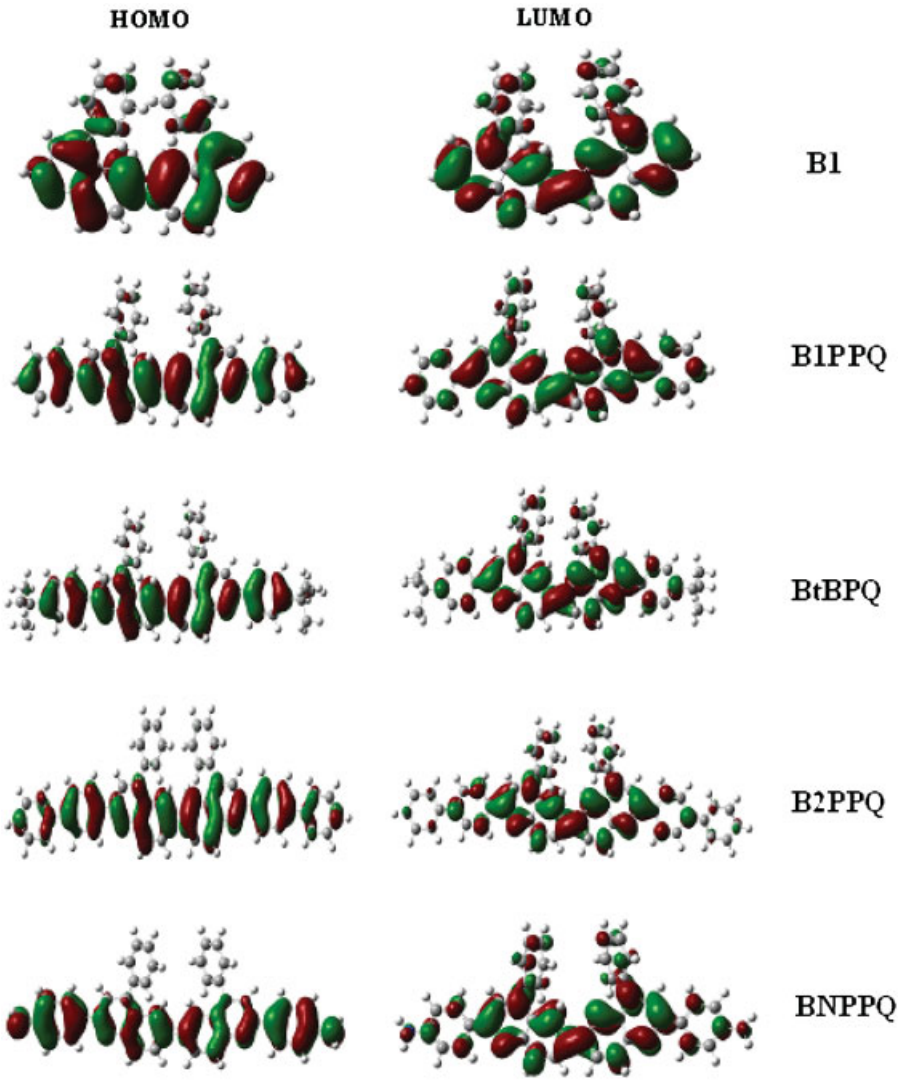

Figure 3. HOMO and LUMO orbitals of B1, BQPPQ, BtBPQ, B2PPQ, and BNPPQ by B3LYP/6-31G

the bridge carbon atom and its conjoint atoms of the intra-ring in the HOMO. On the contrary, there is bonding in the bridge single bond of the inter-ring and antibonding between the bridge atom and its neighbor in the intra-ring in the LUMO. This may explain the nonplanarity that is observed for these oligomers in their ground states. However, the LUMO of all of the oligomers generally shows bonding character between the two adjacent subunits. This can implies that the singlet excited state involving mainly the promotion of an electron from the HOMO to the LUMO should be more planar.

The HOMO and LUMO energies can be calculated nicely by DFT in this study. The energies of HOMO and LUMO orbitals have been complied in Fig. 4. As shown in Fig. 4, the HOMO energy levels are ∼−5.89, ∼−5.64, ∼−5.52, ∼−5.53, and ∼−4.90 eV in B1, B1PPQ, BtBPQ, B2PPQ, and BNPPQ, respectively. The HOMO energy level of BNPPQ is higher than the energies of all the other molecules, indicating that the presence of the aniline groups on the 4-phenyl-6-(4-phenylquinolin-6-yl)quinoline core have significantly improved the hole-creating properties of the oligomers. Additionally, the LUMO energy levles slightly change in B1 (−1.80 eV), B1PPQ (−1.91 eV), BtBPQ (−1.84 eV), and B2PPQ (−1.94 eV), suggesting that these four aryl substituents does not effect much on the electron-accepting ability. It is noteworthy that the LUMO of BNPPQ (−1.56 eV) sharply increases about 0.3 eV less than the four molecules above. This is reasonable because the HOMO shows inter-ring antibonding character and

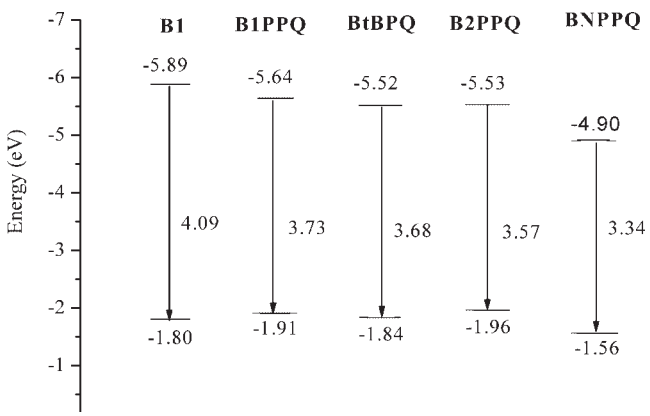

Figure 4. The calculated HOMO, LUMO energy levels (in eV), and the HOMO–LUMO gaps (Δ_{H-L}) of each molecular by B3LYP/6-31G

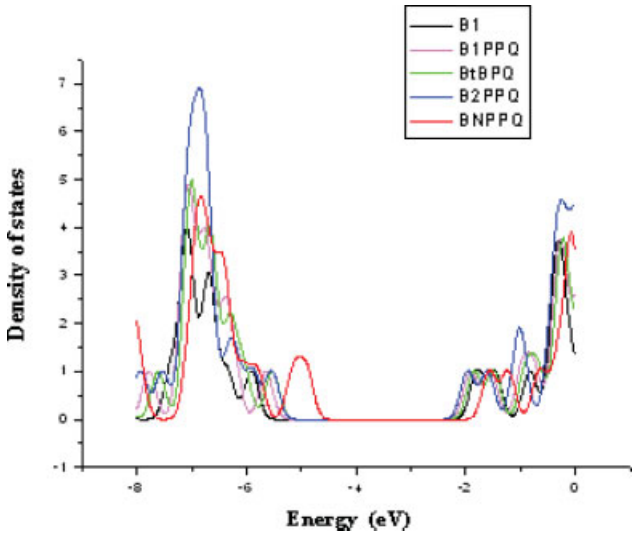

Figure 5. Total of DOS of B1, B1PPQ, BtBPQ, B2PPQ, and BNPPQ

the LUMO shows inter-ring bonding character, the variation of torsional angles should have a larger effect on the LUMO. In a word, BNPPQ is a good hole-creating material.

Furthermore, the total density of states (DOS) of systems B1, B1PPQ, BtBPQ, B2PPQ, and BNPPQ which were carried out by B3LYP/6-31G method has been compared in Fig. 5. We can find that the energies of HOMO are similar for B1, B1PPQ, BtBPQ, and B2PPQ, but that of BNPPQ is the highest obviously in these compounds.

HOMO–LUMO gaps and lowest excitation energies

It is well known that the energy gaps are weightily related to the optical and electronic properties. To gain insight into the influence of the various aryl substituents in these five molecules, the calculated HOMO and LUMO energy levels and energy gaps are carried out by B3LYP/6-31G.

In this part, our calculated energy gap in theory is the orbital energy difference between HOMO and LUMO, termed the HOMO–LUMO gap (Δ_{H-L}). Experimentally, it is most obtained from the absorption spectra, which is the lowest transition (or excitation) energy from the ground state to the first dipole-allowed excited state, termed the optical band gap (E_g). In fact, the optical band gap is not the orbital energy difference between HOMO and LUMO, but the energy difference between the S_0 and S_1 states. Only when the excitation to the S_1 state corresponds almost exclusively to the promotion of the electron from the HOMO to the LUMO may the values of the optical band gap and the HOMO–LUMO gap be approximately equal. So, here we also theoretically calculated the optical band gaps of these molecules at TDDFT level. As mentioned above, these optical band gaps are obtained from the absorption spectra.

The HOMO–LUMO gaps and the lowest excitation energies calculated by TDDFT//B3LYP/6-31G as well as counterpart of the experimental data for B1, B1PPQ, BTBPQ, B2PPQ, and BNPPQ in Table 2. The B3LYP/6-31G HOMO–LUMO energy gaps (Δ_{H-L}) are higher than the TDDFT//B3LYP/6-31G energies (E_g). Although there are some discrepancies between the calculated Δ_{H-L} and E_g, the variation trend is similar. As expected, the HOMO–LUMO gaps decrease in the sequence of B1 (4.09 eV), B1PPQ (3.73 eV), BtBPQ (3.68 eV), B2PPQ (3.57 eV), and BNPPQ (3.34 eV) with varying the aryl substituents. The HOMO–LUMO gap of BNPPQ is the narrowest in these five molecules. In Fig. 4, we can vividly observe the variations of the HOMO–LUMO gaps of B1, B1PPQ, BtBPQ, B2PPQ, and BNPPQ. These results presented earlier support that the LUMO, HOMO, and energy gap of these quinoline oligomers can easily be modified or tuned by the use of various substituents at both end of the 4-phenyl-6-(4-phenylquinolin-6-yl)quinoline core. And introducing the electronic donator is a key point toward the development this kind of *n*-type conjugated materials for OLEDs.

Table 2. The HOMO–LUMO gaps (Δ_{H-L}) by B3LYP and the lowest excitation energies (E_gs) (in eV) by TDDFT of each molecular

Molecular	Δ_{H-L}	E_gs (TD)	E_gs[7] (expl)
B1	4.09	3.69	—
B1PPQ	3.73	3.35	3.0
BtBPQ	3.68	3.29	3.0
B2PPQ	3.57	3.19	2.85
BNPPQ	3.34	3.00	—

Ionization potentials and electron affinities

The device performance of OLEDs depends on the charge injection and transport as well as the excitation confinement in a device. In this section, we present the calculated IPs and EAs by DFT//B3LYP/6-31G for B1, B1PPQ, BtBPQ, B2PPQ, and BNPPQ in Table 3.

Herein, we list IP and EA either for vertical (v: at the geometry of the neutral molecule) or adiabatic (a: optimized structure for both the neutral and charged molecule). The variety trends of the IP and EA for each molecule are similar to those of the negative of HOMO and LUMO energies. The energies required to create a hole for B1, B1PPQ, BtBPQ, B2PPQ, and BNPPQ are 7.07, 6.53, 6.26, 6.26, and 5.71 eV, respectively, whereas the extraction of an electron from the anion require 0.73, 0.99, 0.95, 1.12, and 0.66 eV, respectively. It is clear that the calculated IP is decreasing by the use of various substituents at both ends. At the same time, our calculated EA values increase in the sequence of B1, BtBPQ, B1PPQ, BNPPQ, and B2PPQ. In a word, the IP value of BNPPQ is the lowest in these five oligomers and the EA value of B2PPQ is the highest. Obviously, introducing the aminobenzene group at the main core can improve the ability to create holes, which is in accord with the analysis from the HOMO and LUMO energies. This should be useful to enhance the injection of holes and electron transport from anode and cathode in light-emitting diodes.

Table 3. IPs and EAs for each molecular (in eV)

Molecular	IP (a)	IP (v)	EA (a)	EA (v)
B1	7.07	7.07	0.73	0.55
B1PPQ	6.53	6.80	0.99	0.87
BtBPQ	6.26	6.53	0.95	0.83
B2PPQ	6.26	6.26	1.12	1.02
BNPPQ	5.71	5.71	0.66	0.54

Table 4. Absorption spectra data obtained by the TDDFT//B3LYP/6-31G on the DFT//B3LYP/6-31G geometries for each molecular

Electronic transitions	Wavelengths (nm)	*f*	MO/character	Coefficient
B1				
$S_0 \rightarrow S_1$	335.85	0.1599	HOMO → LUMO	0.66
$S_0 \rightarrow S_2$	318.59	0.0260	HOMO → LUMO+1	0.58
$S_0 \rightarrow S_3$	313.57	0.0047	HOMO−3 → LUMO	0.53
B1PPQ				
$S_0 \rightarrow S_1$	370.63	0.7888	HOMO → LUMO	0.67
$S_0 \rightarrow S_2$	339.39	0.0180	HOMO → LUMO+1	0.62
$S_0 \rightarrow S_3$	321.74	0.0232	HOMO-2 → LUMO	0.44
Experiment BtBPQ	356[a], 369[b]			
$S_0 \rightarrow S_1$	376.77	1.0111	HOMO → LUMO	0.67
$S_0 \rightarrow S_2$	343.20	0.0178	HOMO → LUMO+1	0.64
$S_0 \rightarrow S_3$	323.58	0.0265	HOMO−2 → LUMO	0.50
Experiment B2PPQ	360[a], 370[b]			
$S_0 \rightarrow S_1$	388.67	1.4718	HOMO → LUMO	0.67
$S_0 \rightarrow S_2$	348.80	0.0110	HOMO → LUMO+1	0.64
$S_0 \rightarrow S_3$	341.38	0.0008	HOMO−1 → LUMO	0.67
Experiment BNPPQ	366[a], 384[b]			
$S_0 \rightarrow S_1$	412.93	1.0256	HOMO → LUMO	0.67
$S_0 \rightarrow S_2$	376.56	0.0004	HOMO−1 → LUMO	0.62
$S_0 \rightarrow S_3$	372.61	0.0100	HOMO → LUMO+1	0.63

[a] Measured in dilute solution.
[b] Measured as thin films in ref. 7, 8.

Absorption spectra

We have obtained the absorption spectra of the singlet–singlet electronic transition of B1, B1PPQ, BtBPQ, B2PPQ, and BNPPQ at TD-DFT//B3LYP/6-31G level. Table 4 lists out the transition energies, oscillator strengths and main configurations for the most relevant first three singlet excited states by TD-DFT.

In Table 4, it can be found that our calculated absorption wavelengths by TD-DFT are higher than the experimental results. This discrepancy may be owing to neglecting completely the solvent effects. However, the results can still reflect some variation trend. Obviously, this excitation to the S_1 state corresponds all exclusively to the promotion of an electron from HOMO to LUMO. The oscillator strength (f) of the $S_0 \rightarrow S_1$ electronic transition is the largest in each molecule except B1. Moreover, we also find that with the variety of the substituents on the central core, the absorption wavelengths increase in the sequence of B1, B1PPQ, BtBPQ, B2PPQ, and BNPPQ, presenting the red shifts both in experiment and calculation. Our calculated absorption spectra data are 335.85 (B1) < 370.63 (B1PPQ) < 376.77 (BtBPQ) < 388.67 (B2PPQ) < 412.93 nm (BNPPQ), which have the same trend compared with the experimental absorption spectra [369 (B1PPQ) < 370 (BtBPQ) < 384 nm (B2PPQ) measured as thin films[7,8]]. This is reasonable because the HOMO → LUMO transition is predominant in the $S_0 \rightarrow S_1$ electronic transition and, as the analysis above shows, with the extension of the π-conjugated area or introduction of the electronic donator on the central core, the HOMO–LUMO gaps decrease.

Emission spectra and the decay lifetimes

In this article, TD-DFT//B3LYP/6-31G has used on the basis of the optimized excited state geometry to obtain the emission wavelengths for these five quinoline derivatives under study. These calculated outcomes show that on going from B1, B1PPQ, BtBPQ, B2PPQ, and BNPPQ, the emission wavelengths exhibit red shift [391.48 < 430.07 < 435.86 < 444.57 < 463.28 nm see in Table 5]. The Stoke's shifts are 55.63, 59.44, 59.09, 55.9, and 50.35 nm, respectively. The Stoke's shifts of these five oligomers are similar, and that of BNPPQ is the smallest. This may be because of introducing the aminobenzene group which is electron donator on the central core. Furthermore, similar to the absorption spectra, the emission peaks with the strongest oscillator strength are all assigned to $\pi \rightarrow \pi^*$ character arising from HOMO to LUMO transition in these five oligomers.

Moreover, to further explore the nature of the emitting excited states of these five oligomers, we calculated the decay lifetimes. On the basis of the fluorescence energy and oscillator strength,[24–26] the radiative lifetimes (τ) have been computed for spontaneous emission by using the Einstein transition probabilities according to the formula (in au)[24,27] as follow:

$$\tau = \frac{C^3}{2(E_{Flu})^2 f}$$

where *C* is the velocity of light, E_{Flu} is the transition energy, and *f* is the oscillator strength. The calculated lifetime τ for these five molecules and the experimental data are listed in Table 5 by TD-DFT method. The variation of substituents leads to decrease of excitation energies and an increase in oscillator strengths, but a sharp decrease in oscillator strength in BNPPQ. These cause a decrease of calculated radiative lifetime (τ) except for BNPPQ (see in Table 5). The experimental values for B1PPQ, BtBPQ, and B2PPQ were measured in dilute solution, whereas our data in this work were all calculated as gassiest. So there are some discrepancies between the calculated values and the experimental data. However, it is obviously that the general variation direction is

Table 5. Emission spectra data obtained by the TDDFT//B3LYP/6-31G based on the CIS/6-31G geometries for each molecular

Molecule	Electronic transition	Wavelengths (nm)	f	τ (ns)	MO/character	Experimental wavelengths (nm)	
B1	$S_1 \rightarrow S_0$	391.48	0.3144	5.66	HOMO → LUMO	—	—
B1PPQ	$S_1 \rightarrow S_0$	430.11	1.1371	2.46	HOMO → LUMO	401[a]	440[b]
BtBPQ	$S_1 \rightarrow S_0$	435.87	1.3818	2.07	HOMO → LUMO	405[a]	443[b]
B2PPQ	$S_1 \rightarrow S_0$	444.57	1.7698	1.69	HOMO → LUMO	409[a]	458[b]
BNPPQ	$S_1 \rightarrow S_0$	463.28	1.4557	2.23	HOMO → LUMO	—	—

[a] Measured in dilute solution.
[b] Measured as thin films in ref. 7, 8.

similar either in experiment or in calculation. All in all, the calculated lifetimes match fairly well with the experimental data for the blue emission.

CONCLUSIONS

A systematic theoretical study has been performed on *n*-type conjugated oligomers in this work. The frontier molecular orbitals were spread over the backbone. The HOMO possesses an antibonding character and the LUMO holds a bonding character between the two adjacent subunits, which may explain that the excited-state structures of each molecule have a better coplanar conformation than the ground-state structures. Importantly, the introduction of better electron-donating groups on the central core can increase the HOMO energies; consequently, this should be useful to enhance the injection of holes. Excitation to the S_1 state corresponds almost exclusively to the promotion of an electron from HOMO to LUMO. Varying the substituents leads to a red shift of the absorption peak in the sequence of B1, B1PPQ, BtBPQ, B2PPQ, and BNPPQ. In addition, the emission of these five molecules also appear red-shifted to some extent.

Overall, these five *n*-type oligoquinolines derivatives are excellent materials for further development as robust blue emitters for blue OLEDs. And it is remarkable that BNPPQ is the better choice as hole-transport materials in the oligomers we investigated.

Acknowledgements

This work was funded by Major State Basis Research Development Program 2002CB 613406, National Nature Science Foundation of China 20673045, and Key Laboratory for Superamolecular Structure and Material of Jilin University.

REFERENCES

[1] Y. Kishigami, K. Tsubaki, Y. Kondo, J. Kido, *Synth. Met.* **2005**, *153*, 241–244.
[2] M. T. Lee, C. H. Liao, C. H. Tsai, C. H. Chen, *Adv. Mater.* **2005**, *17*, 2493–2497.
[3] B. K. Shah, D. C. Neckers, J. Shi, E. W. Forsythe, D. Morton, *Chem. Mater.* **2006**, *18*, 603–608.
[4] C. Hosokawa, H. Higashi, H. Nakamura, T. Kusumoto, *Appl. Phys. Lett.* **1995**, *67*, 3853–3855.
[5] J. Shi, C. W. Tang, *Appl. Phys. Lett.* **2002**, *80*, 3201–3203.
[6] R. Y. Wang, W. Li., Jia, H. Aziz, G. Vamvounis, S. Wang, N. X. Hu, Z. D. Popović, J. A. Coggan, *Adv. Funct. Mater.* **2005**, *15*, 1483–1487.
[7] C. J. Tonzola, A. P. Kulkarni, A. P. Gifford, W. Kaminsky, S. A. Jenekhe, *Adv. Funct. Mater.* **2007**, *17*, 863–874.
[8] A. P. Kulkarni, A. P. Gifford, C. J. Tonzola, S. A. Jenekhe, *Appl. Phys. Lett.* **2005**, *86*, 061106.
[9] X. Zhang, A. S. Shetty, S. A. Jenekhe, *Macromolecules* **1999**, *32*, 7422–7429.
[10] Y. Zhu, M. M. Alam, S. A. Jenekhe, *Macromolecules* **2003**, *36*, 8958–8968.
[11] C. J. Tonzola, M. M. Alam, B. A. Bean, S. A. Jenekhe, *Macromolecules* **2004**, *37*, 3554–3563.
[12] T. W. Kwon, M. M. Alam, S. A. Jenekhe, *Chem. Mater.* **2004**, *16*, 4657–4666.
[13] L. Yang, Y. Liao, J. K. Feng, A. M. Ren, *J. Phys. Chem. A* **2005**, *109*, 7764–7774.
[14] L. Yang, J. K. Feng, A. M. Ren, *J. Org. Chem.* **2005**, *70*, 5987–5996.
[15] L. Yang, A. M. Ren, J. K. Feng, J. F. Wang, *J. Org. Chem.* **2005**, *70*, 3009–3020.
[16] L. Yang, J. K. Feng, A. M. Ren, C. C. Sun, *Polymer* **2006**, *47*, 3229–3239.
[17] G. C. Yang, T. Su, S. Q. Shi, Z. M. Su, H. Y. Zhang, Y. Wang, *J. Phys. Chem. A* **2007**, *111*, 2739–2744.
[18] Y. L. Liu, J. K. Feng, A. M. Ren, *J. Comput. Chem.* **2007**, *28*, 2500–2509.
[19] B. C. Lin, C. P. Cheng, Z. P. Lao, *J. Phys. Chem. A* **2003**, *107*, 5241–5251.
[20] J. F. Wang, J. K. Feng, A. M. Ren, X. D. Liu, Y. G. Ma, P. Lu, H. X. Zhang, *Macromolecules* **2004**, *37*, 3451–3458.
[21] P. Crostrand, Z. Rinkevicius, Y. Luo, H. Agren, *J. Chem. Phys.* **2005**, *122*, 224104.
[22] P. C. Jha, E. Jansson, H. Agren, *Chem. Phys. Lett.* **2006**, *424*, 23–27.
[23] M. J. Frisch, G. W. Trucks, H. B. Schlegel, G. E. Scuseria, M. A. Robb, J. R. Cheeseman, J. A. Montgomery, J. T. Vreven, K. N. Kudin, J. C. Burant, J. M. Millam, S. S. Iyengar, J. Tomasi, V. Barone, B. Mennucci, M. Cossi, G. Scalmani, N. Rega, G. A. Petersson, H. Nakatsuji, M. Hada, M. Ehara, K. Toyota, R. Fukuda, J. Hasegawa, M. Ishida, T. Nakajima, Y. Honda, O. Kitao, H. Nakai, M. Klene, X. Li, J. E. Knox, H. P. Hratchian, J. B. Cross, C. Adamo, J. Jaramillo, R. Gomperts, R. E. Stratmann, O. Yazyev, A. J. Austin, R. Cammi, C. Pomelli, J. W. Ochterski, P. Y. Ayala, K. Morokuma, G. A. Voth, P. Salvador, J. J. Dannenberg, V. G. Zakrzewski, S. Dapprich, A. D. Daniels, M. C. Strain, O. Farkas, D. K. Malick, A. D. Rabuck, K. Raghavachari, J. B. Foresman, J. V. Ortiz, Q. Cui, A. G. Baboul, S. Clifford, J. Cioslowski, B. B. Stefanov, G. Liu, A. Liashenko, P. Piskorz, I. Komaromi, R. L. Martin, D. J. Fox, T. Keith, M. A. Al-Laham, C. Y. Peng, A. Nanayakkara, M. Challacombe, P. M. W. Gill, B. Johnson, W. Chen, M. W. Wong, C. Gonzalez, J. A. Pople, Gaussian 03, Revision B.04; Gaussian, Inc., Pittsburgh, PA, **2003**.
[24] V. Lukeš, A. Aquino, H. Lischka, *J. Phys. Chem. A* **2005**, *109*, 10232–10238.
[25] R. Chidthong, S. Hannongbua, A. J. A. Aquino, P. Wolschann, H. Lischka, *J. Comput. Chem.* **2007**, *28*, 1735–1742.
[26] K. Matuszná, V. Lukeš, P. Rapta, L. Dunsch, A. J. A. Aquino, H. Lischka, *Synth. Met.* **2007**, *157*, 214–221.
[27] I. L. Barzilai, V. Bulatov, V. V. Gridin, I. Schechter, *Anal. Chim. Acta* **2004**, *501*, 151–156.